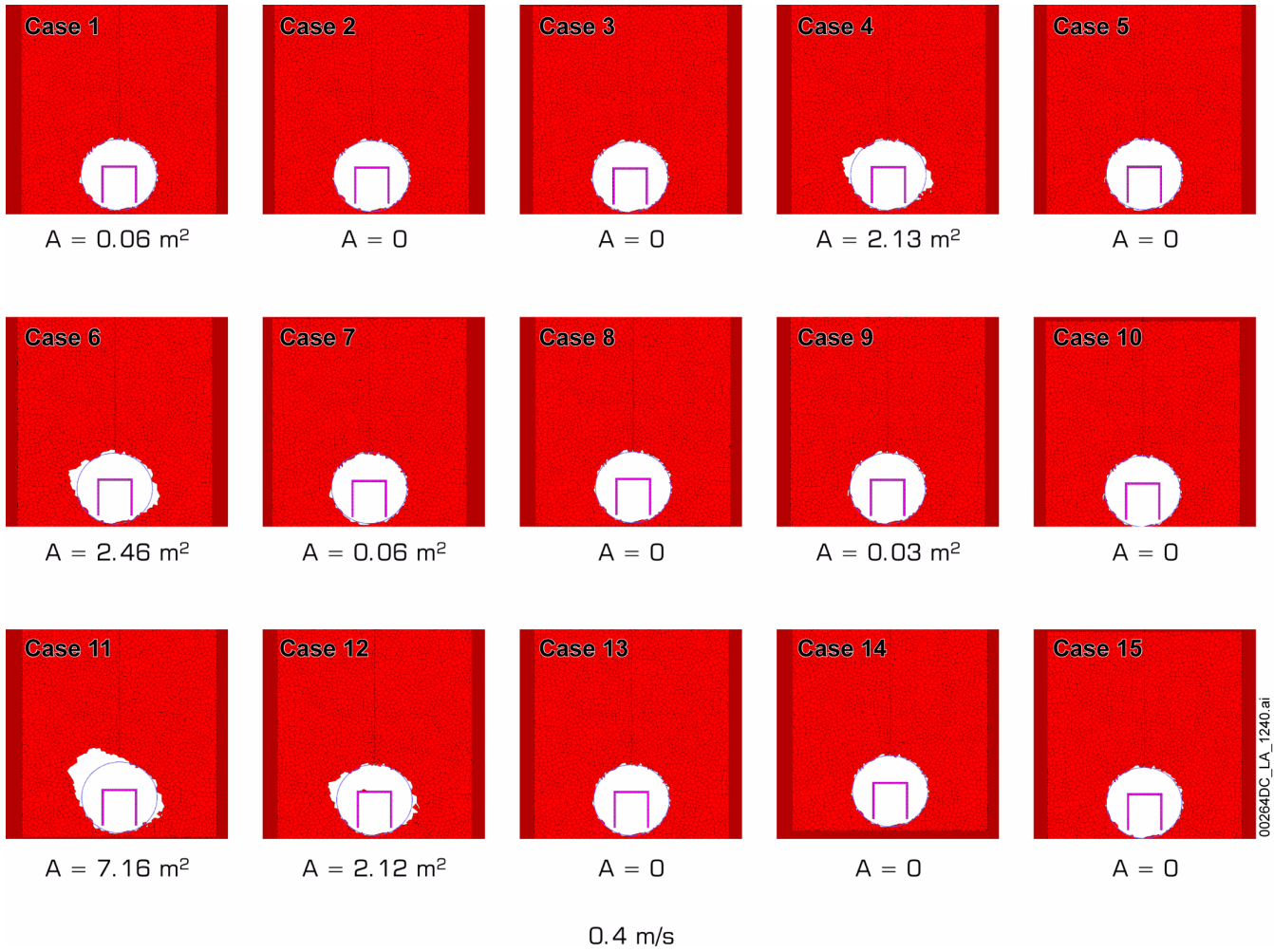

Figure 2.3.3-30. Drift Profiles and Rockfall Volumes (in m^3/m) for Seismic Ground Motion at Horizontal PGV = 0.4 m/s

NOTE: Various cases are shown for different rock categories and ground motion characteristics in lithophysal rock, see Table 2.3.3-5. The dislodged rocks are not depicted in the figure for better illustration of the final drift shapes.

Source: SNL 2007a, Figure 6-2[a].

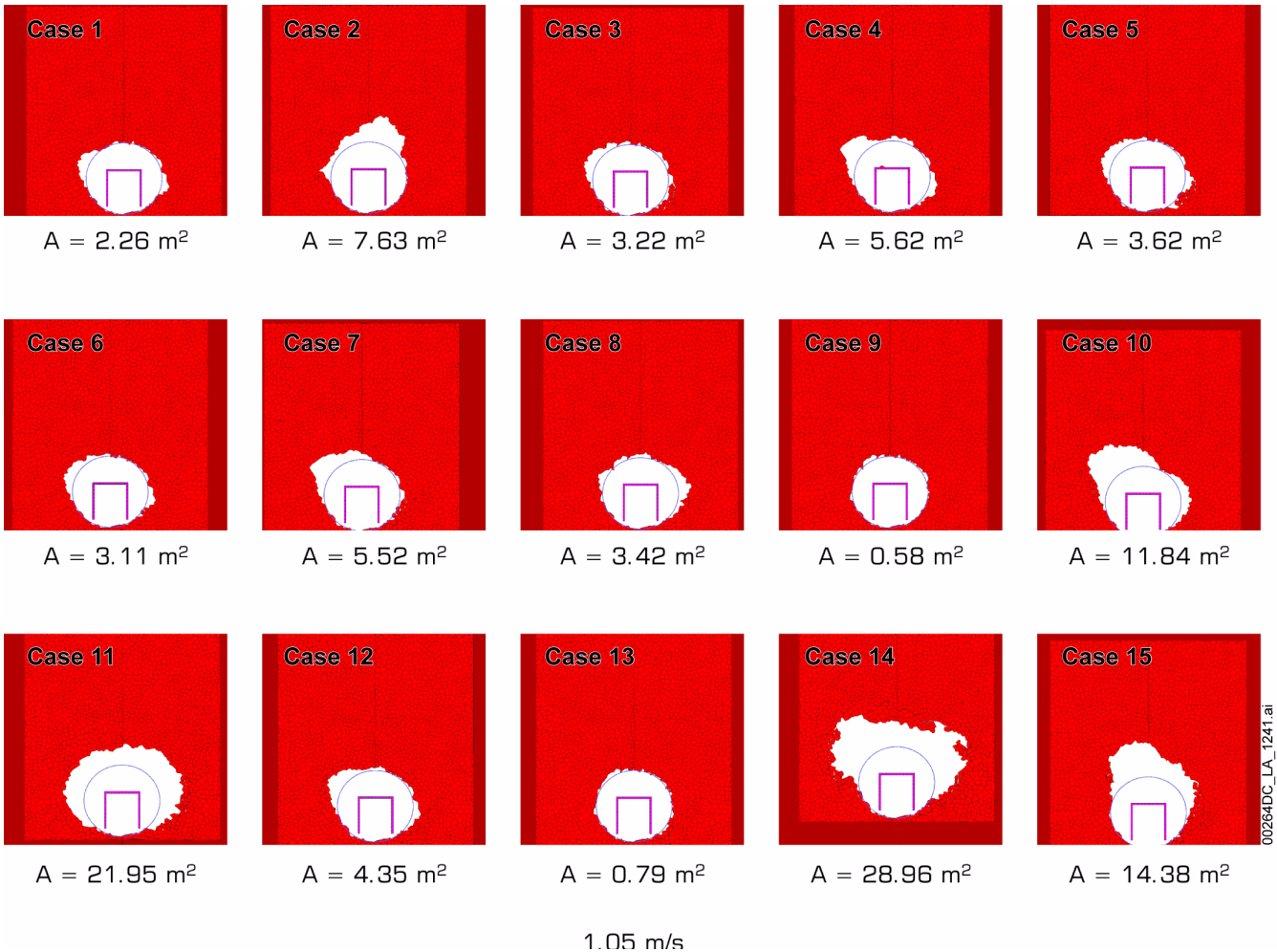

Figure 2.3.3-31. Drift Profiles and Rockfall Volumes (in m^3/m) for Seismic Ground Motion at Horizontal PGV = 1.05 m/s

NOTE: Various cases are shown for different rock categories and ground motion characteristics in lithophysal rock, see Table 2.3.3-5. The dislodged rocks are not depicted in the figure for better illustration of the final drift shapes.

Source: SNL 2007a, Figure 6-3[a].

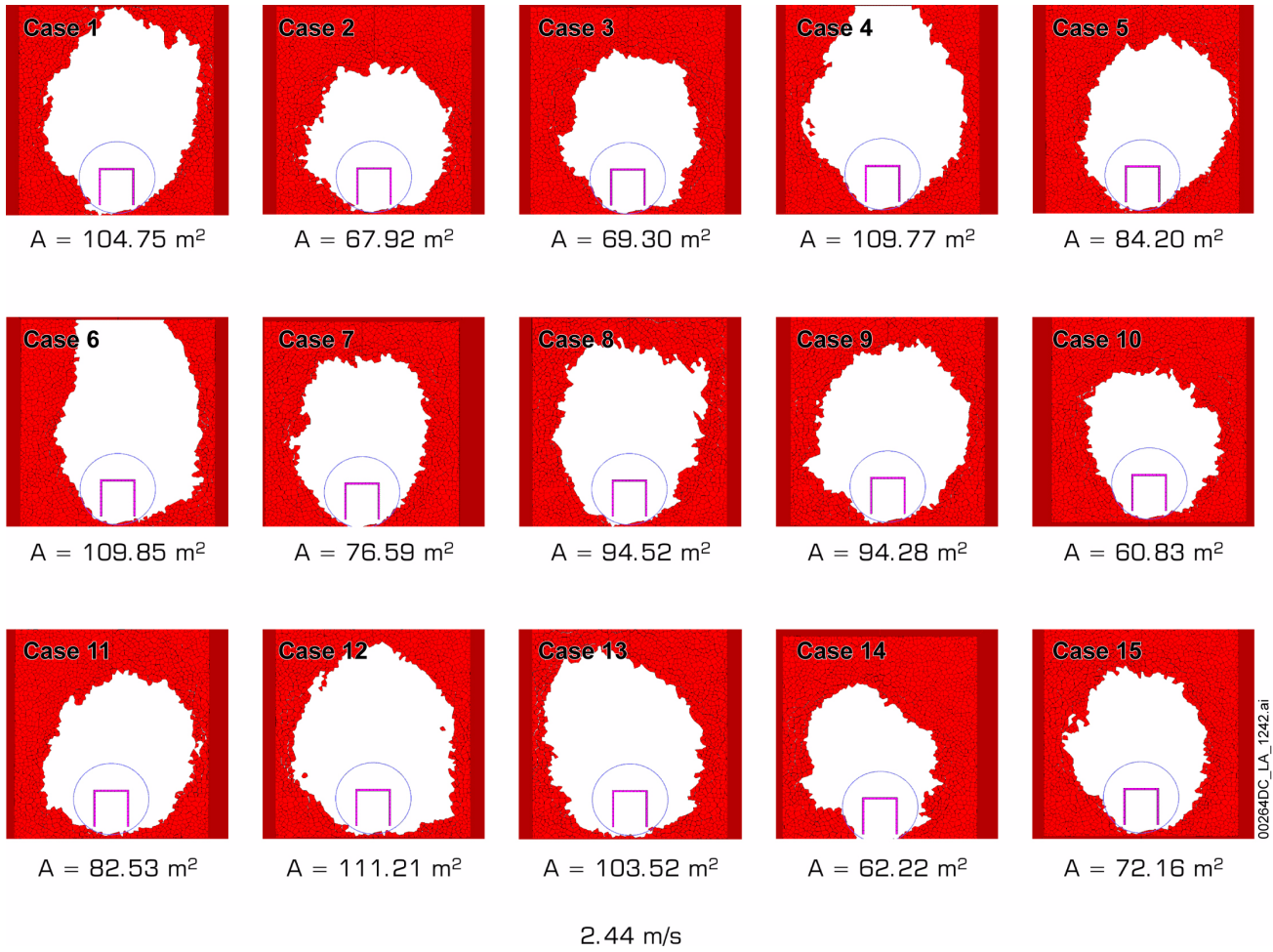

Figure 2.3.3-32. Drift Profiles and Rockfall Volumes (in m^3/m) for Seismic Ground Motion at Horizontal PGV = 2.44 m/s

NOTE: Various cases are shown for different rock categories and ground motion characteristics in lithophysal rock, see Table 2.3.3-5. Dashed circles were added to original figures to illustrate idealized shape of fully collapsed drift in seepage simulations. The dislodged rocks are not depicted in the figure for better illustration of the final drift shapes.

Source: SNL 2007a, Figure 6-4[a].

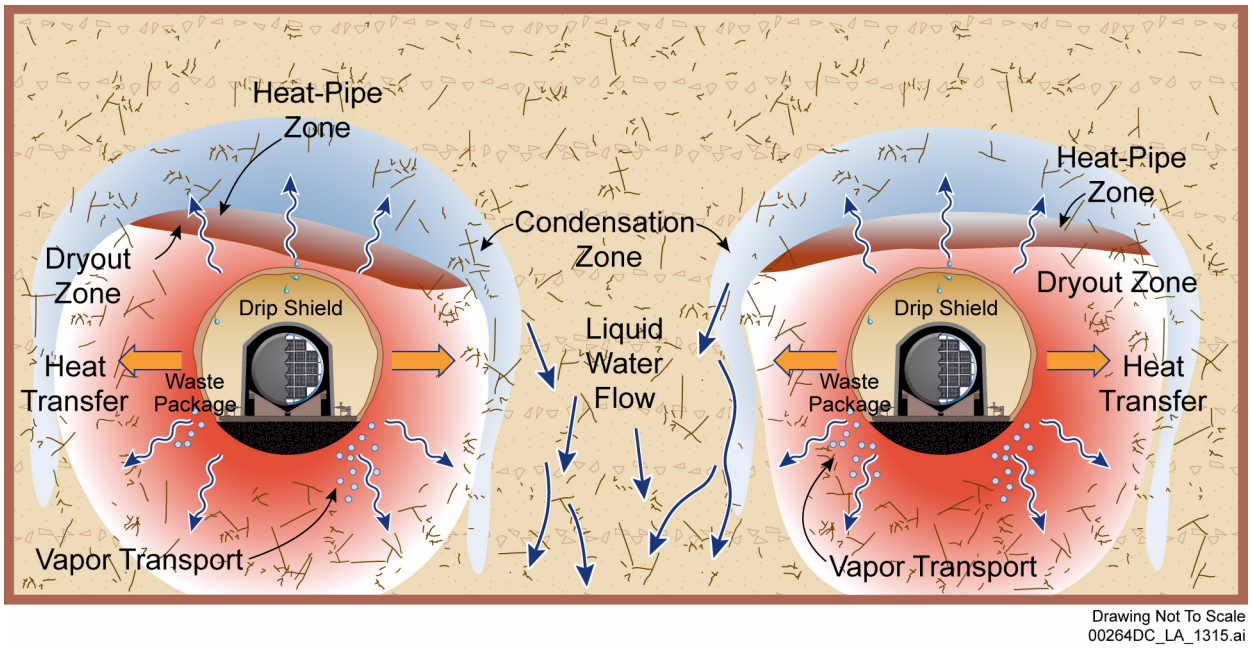

Figure 2.3.3-33. Schematic of Thermal-Hydrologic Processes Occurring in the Emplacement Drift Vicinity as a Result of Repository Heating

Source: Modified from BSC 2005a, Figure 6.1-1 (top).

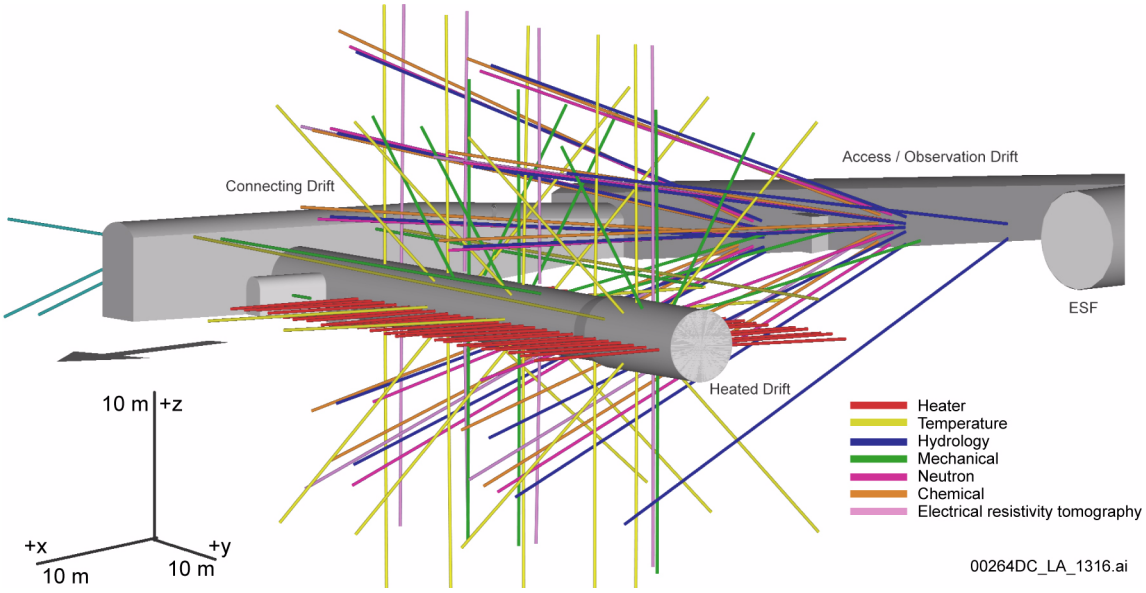

Figure 2.3.3-34. Three-Dimensional Perspective of the As-Built Borehole Configuration of the Drift Scale Test in Alcove 5 (Access/Observation Drift, Connecting Drift, and Heated Drift)

Source: BSC 2005a, Figure 7.2.1-2.

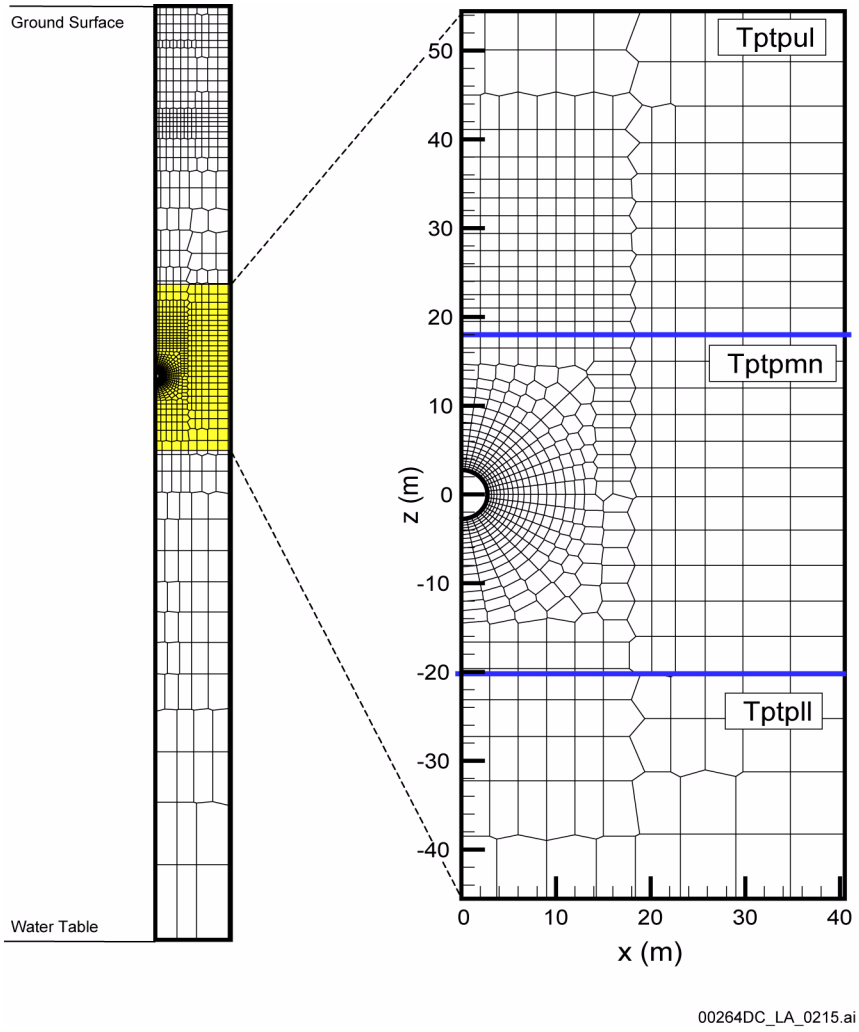

Figure 2.3.3-35. Example of Numerical Grid for the Thermal-Hydrologic Seepage Model

NOTE: The emplacement drift is located in the middle nonlithophysal zone (Tptpmn), which is bounded by the upper lithophysal (Tptpul) and lower lithophysal (Tptpll) zones. The contact between the Tptpmn unit and the Tptpul unit was slightly raised compared to the USW SD-9 data to provide for better continuity at the interface.

Source: Modified from BSC 2005a, Figure 6.2.1.2-1.

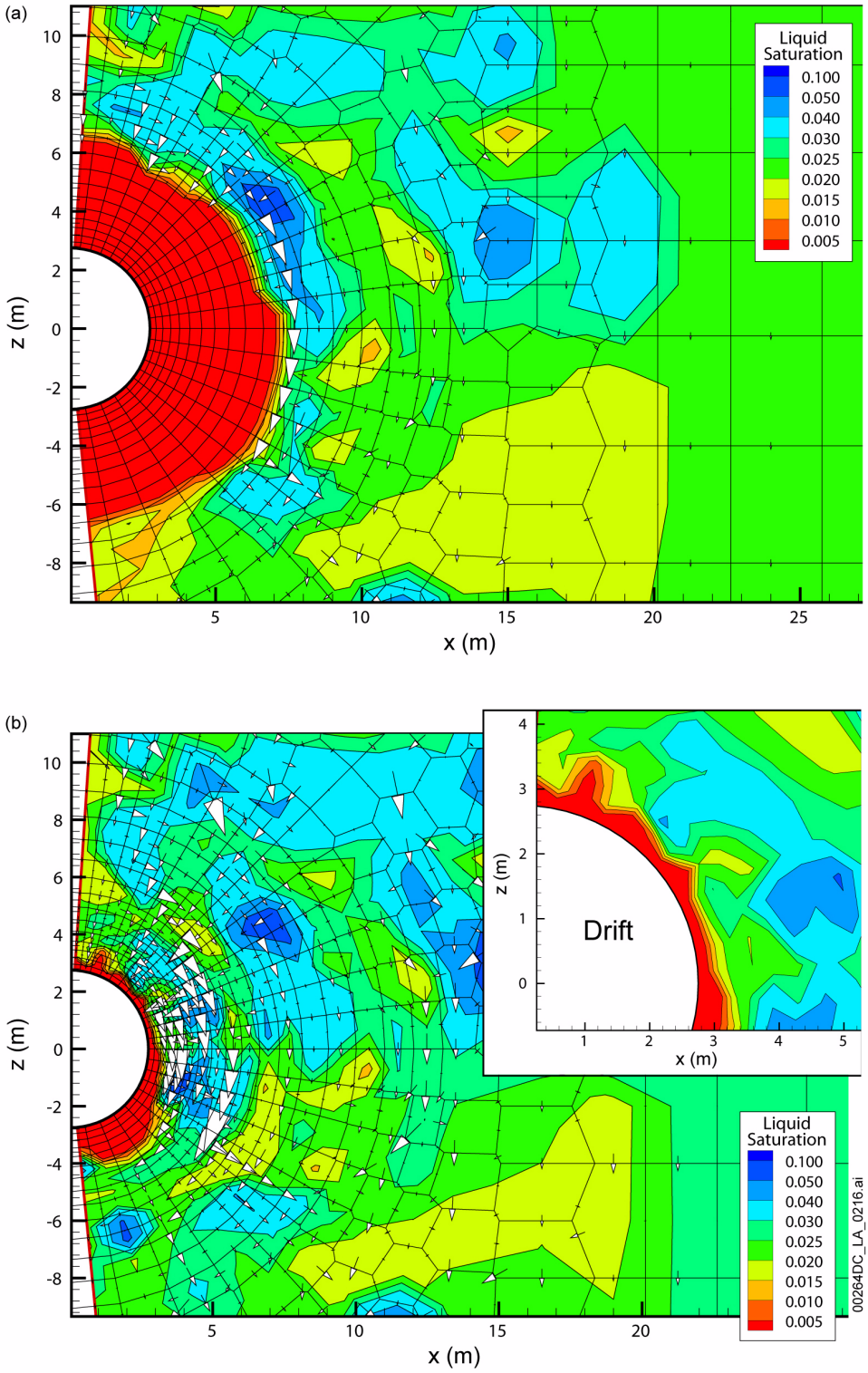

Figure 2.3.3-36. Fracture Saturation and Liquid Flux for the Tptpmn Unit with Heterogeneous Permeability Field at (a) 100 Years and (b) 1,000 Years

Source: BSC 2005a, Figures 6.2.2.2-3a and 6.2.2.2-4a.

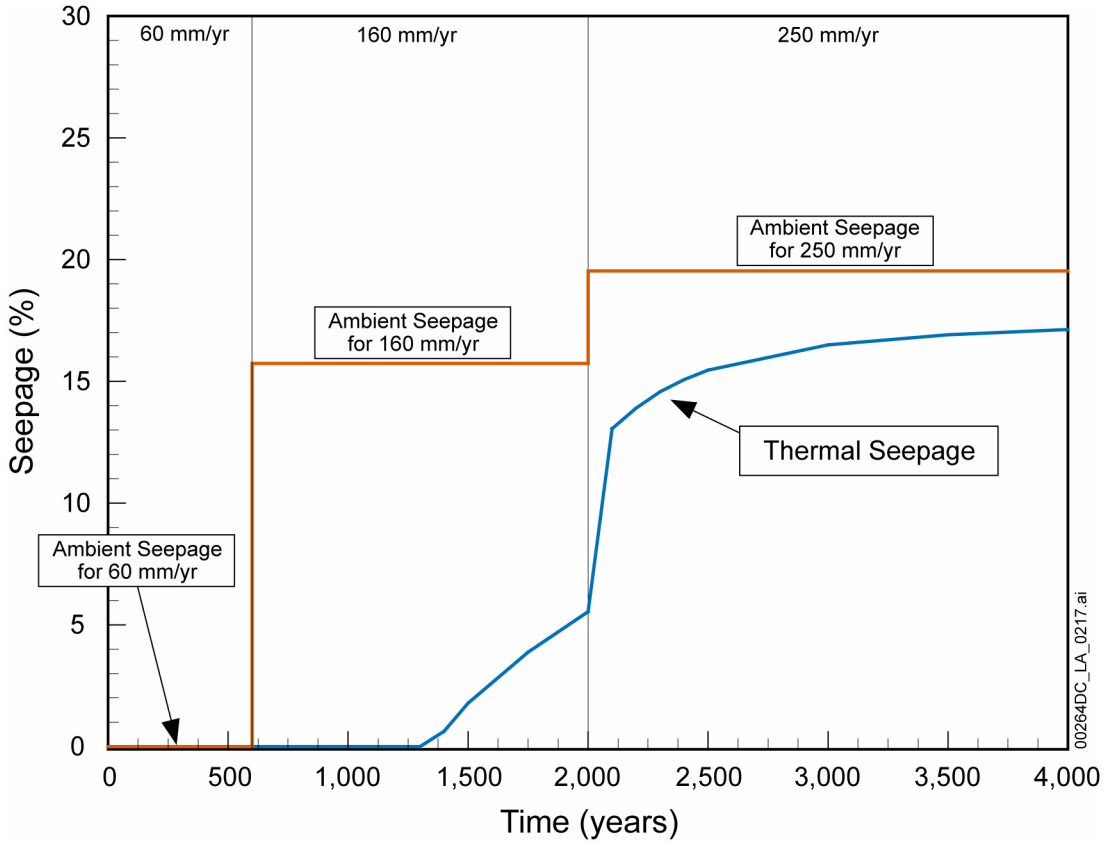

Figure 2.3.3-37. Seepage Percentage for the Tptpmn Unit at Reference Thermal Mode and Tenfold Percolation Flux

NOTE: Percolation flux values shown at top of plot.

Source: BSC 2005a, Figure 6.2.2.2-7b.

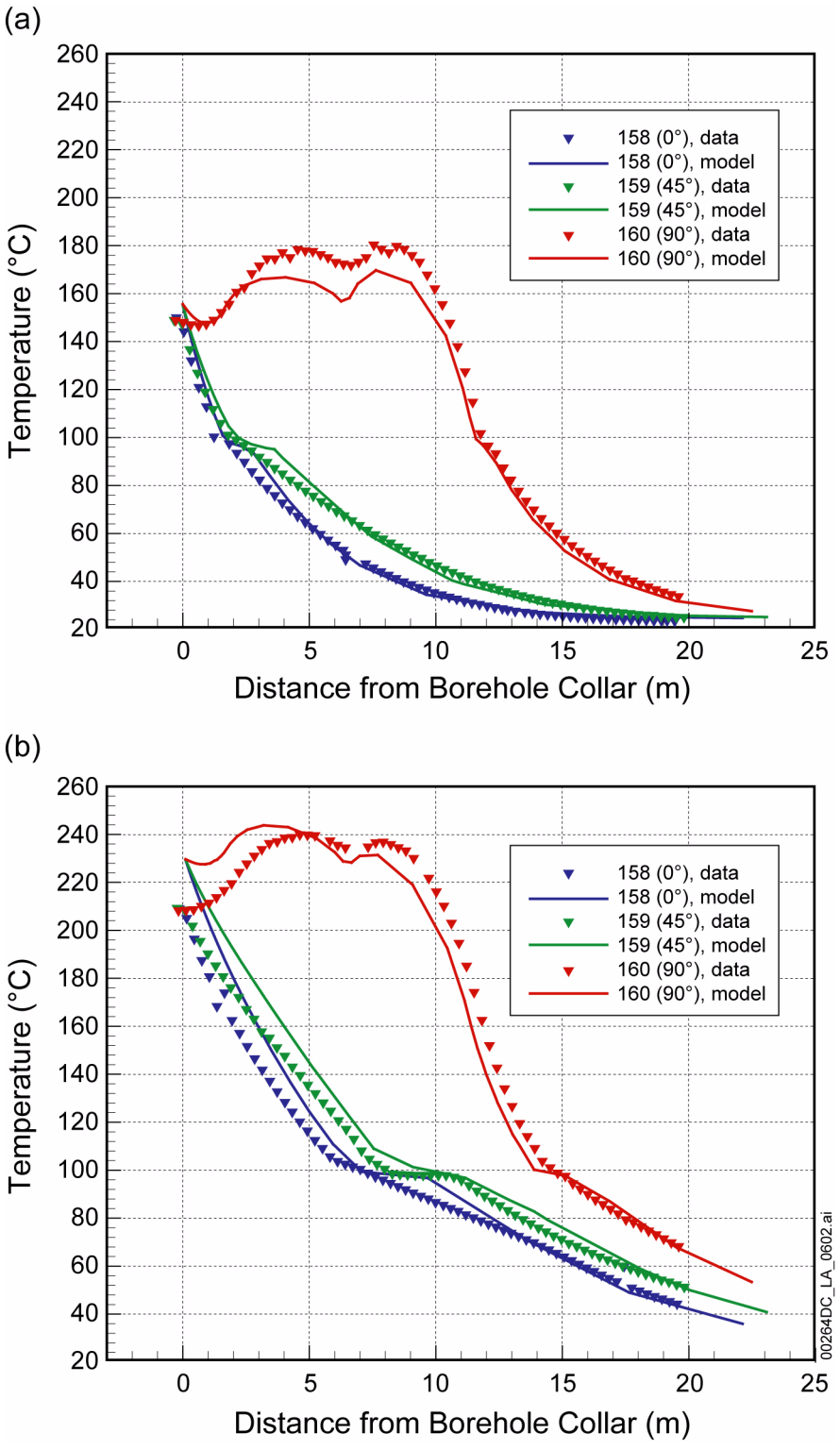

Figure 2.3.3-38. Measured and Simulated Temperature Profile in Boreholes 158, 159, and 160 at Different Times of Heating: (a) 12 months, (b) 48 months

Source: BSC 2005a, Figures 7.4.3.1-1a and 7.4.3.1-1d.

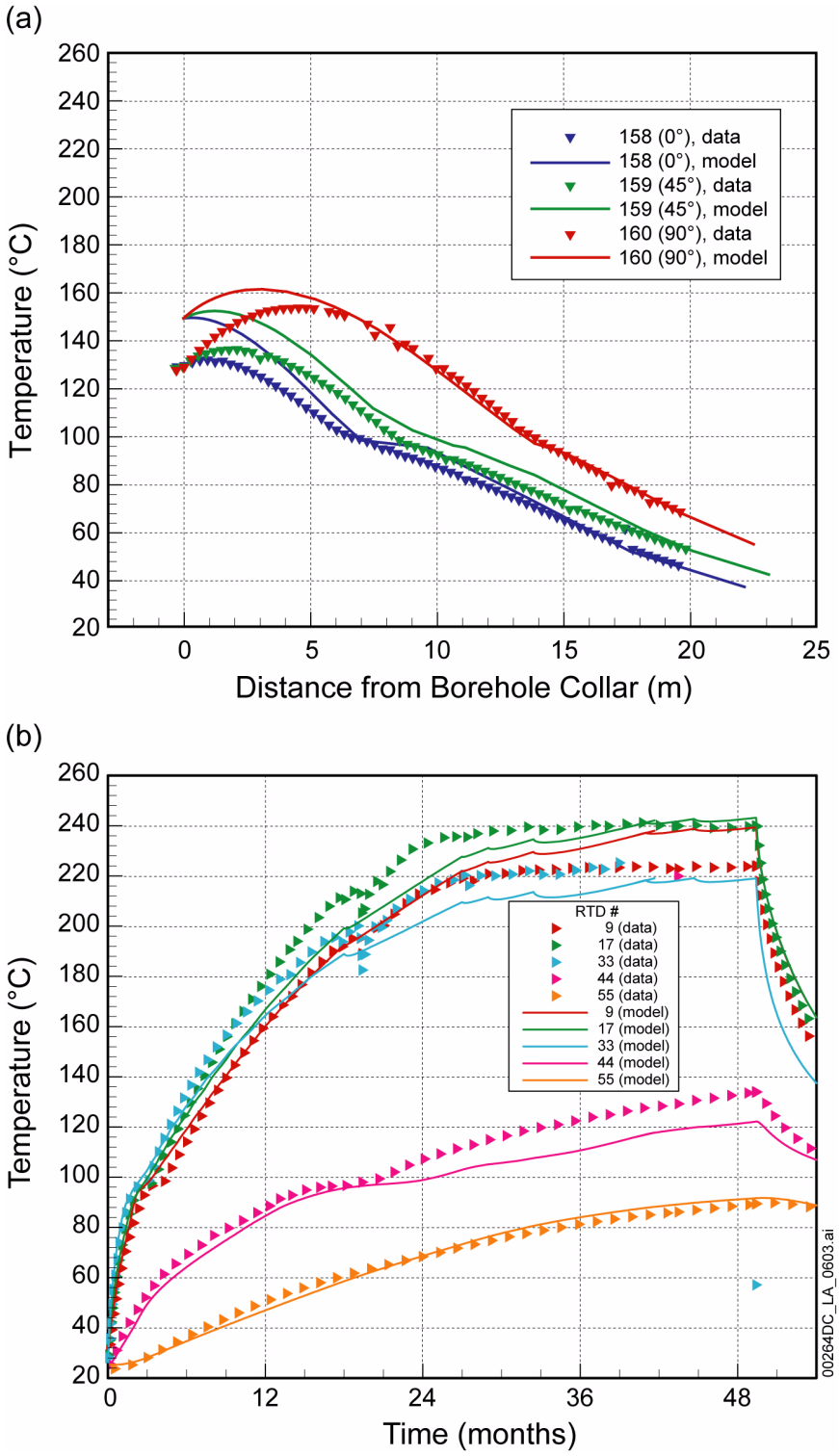

Figure 2.3.3-39. (a) Measured and Simulated Temperature Profile at 5 Months of Cooling in Boreholes 158, 159, and 160 and (b) Temporal Evolution of Temperature in Selected Sensors of Borehole 160

Source: BSC 2005a, Figures 7.4.3.1-2 and 7.4.3.1-3a.

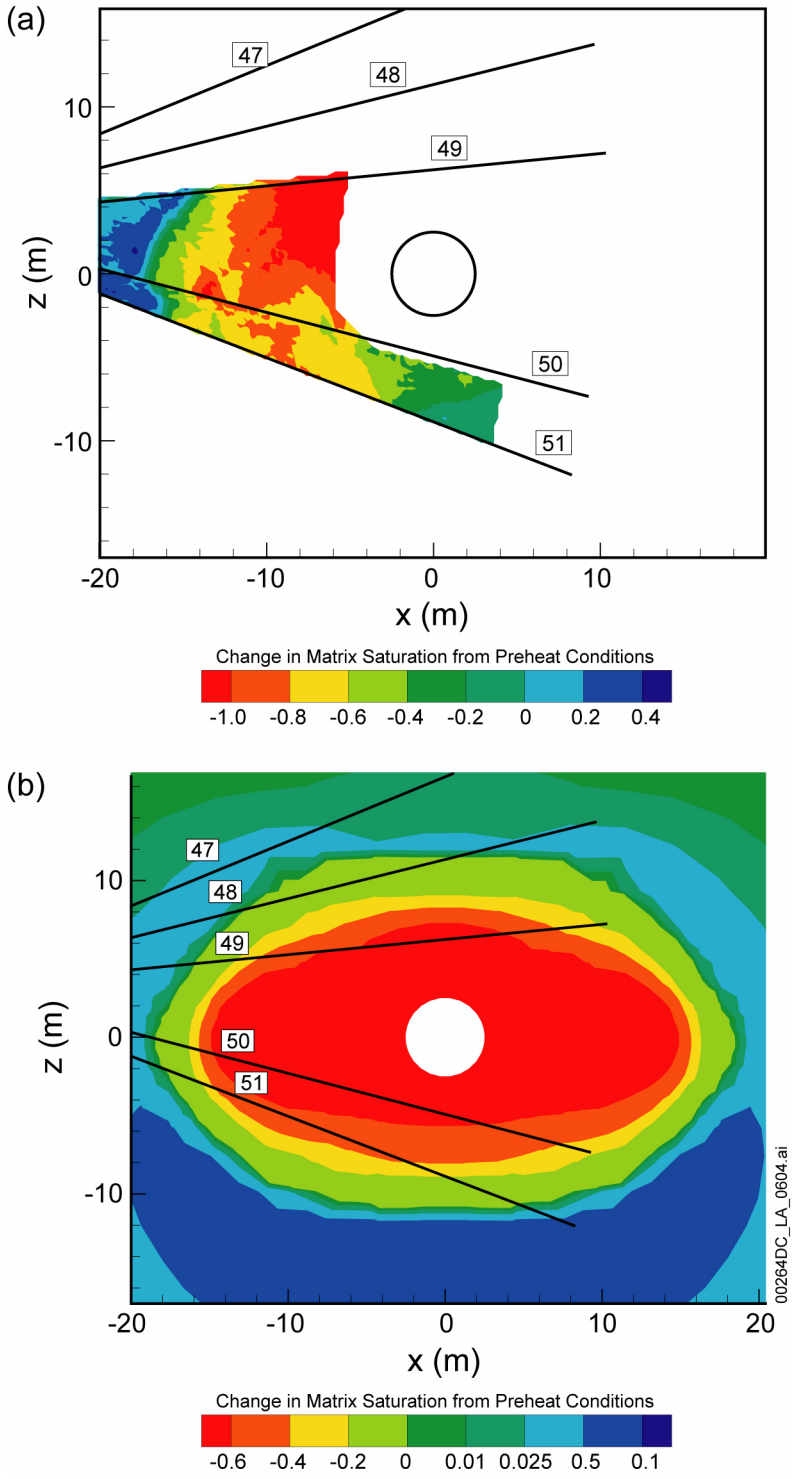

Figure 2.3.3-40. Change in Matrix Liquid Saturation from Preheat Saturation: (a) Measured Ground-Penetrating Radar Data in Boreholes 49 to 51 in January 2002 (Near the End of Heating) and (b) Simulated Change in Matrix Liquid Saturation at End of Heating Phase

Source: BSC 2005a, Figure 7.4.3.2-3.

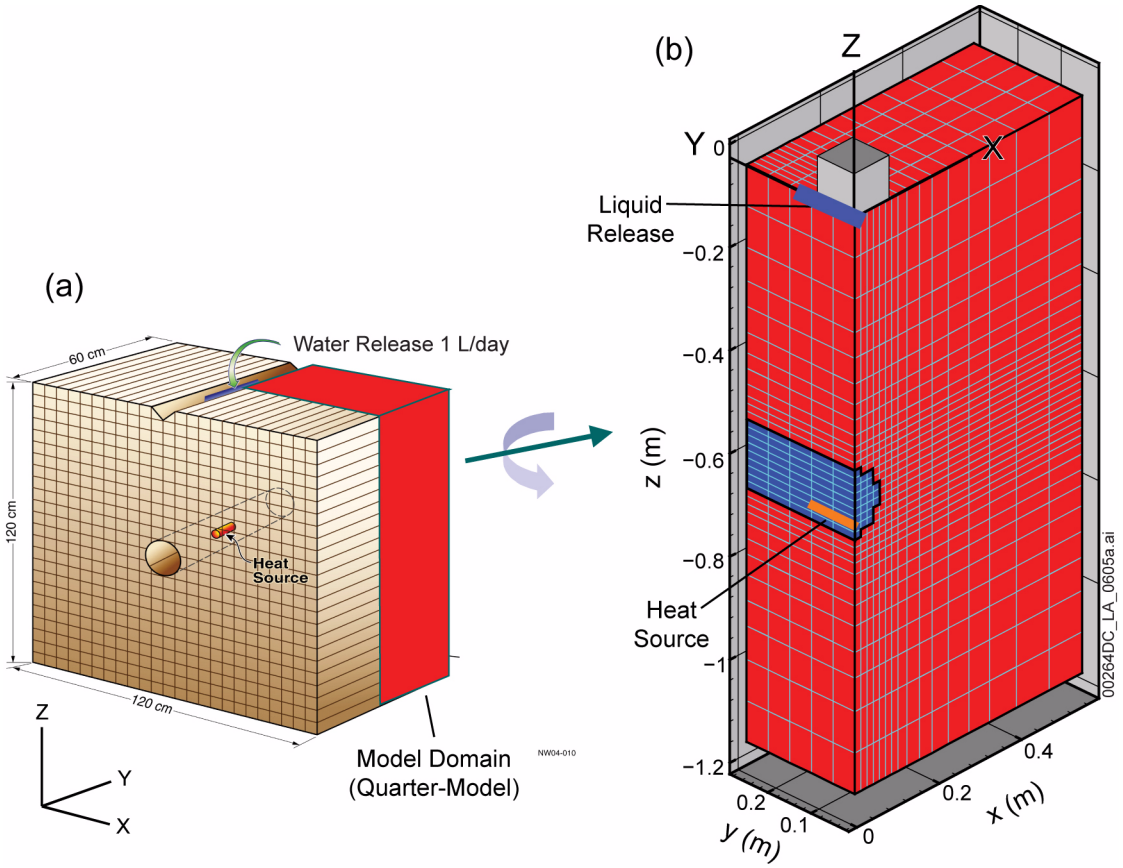

Figure 2.3.3-41. Schematic of (a) Center for Nuclear Waste Regulatory Analyses Heater Experiment and (b) Simulation Domain with Finite Volume Grid

NOTE: The simulation domain reduced to one quarter of the laboratory test cell is rotated around the Z-axis to allow for better visualization.

Source: Birkholzer and Zhang 2006, Figure 3.

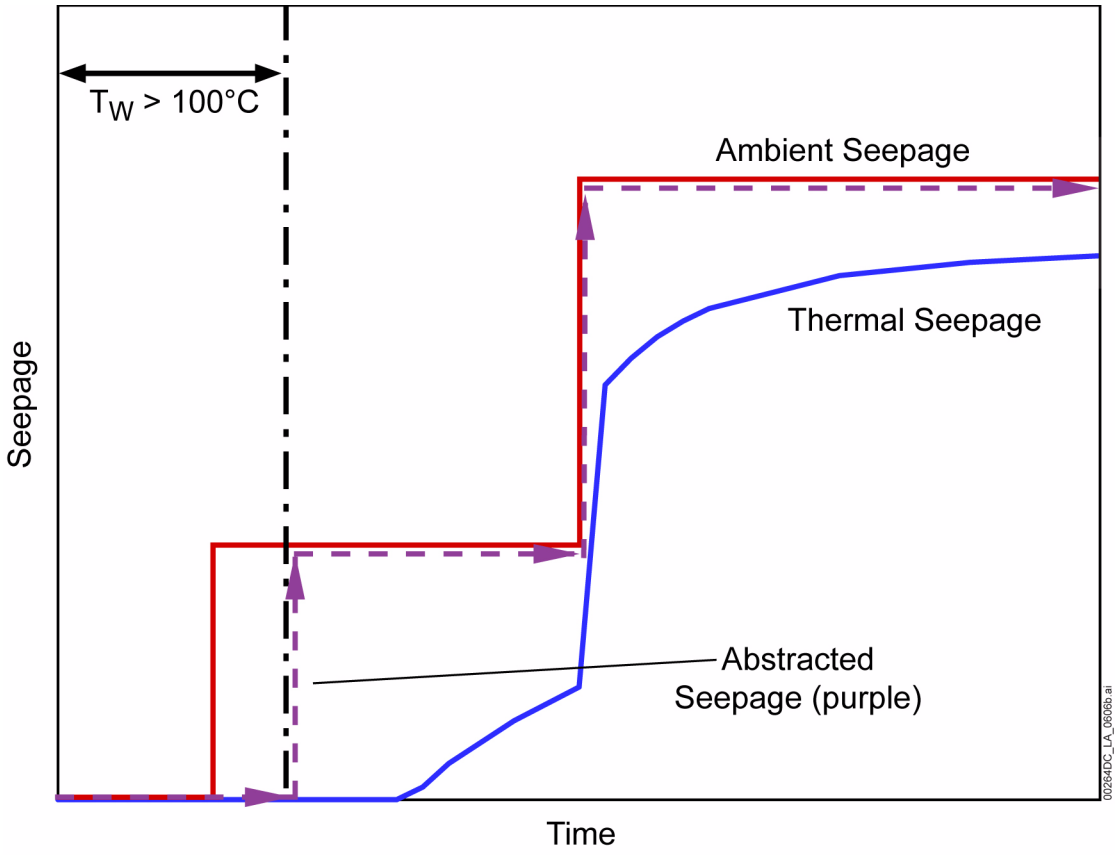

Figure 2.3.3-42. Schematic Illustrating Thermal Seepage Abstraction Method

NOTE: Blue and red lines show simulated thermal and ambient seepage, respectively. Dashed purple line shows abstracted seepage. T_w is drift wall temperature.

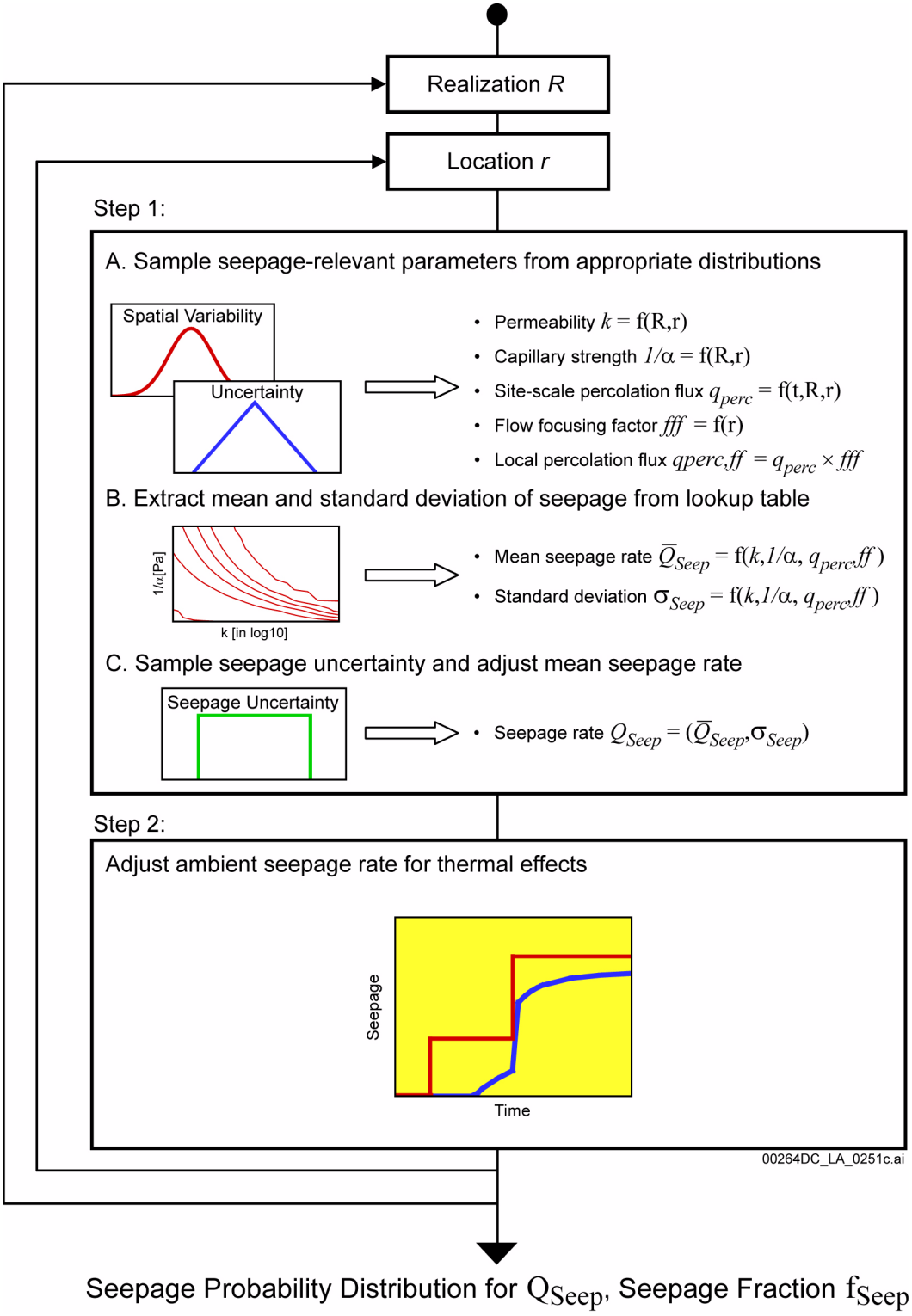

Figure 2.3.3-43. Probabilistic Total System Performance Assessment Procedure for Calculating Seepage at Selected Time Steps (Nominal Scenario)

Source: SNL 2007a, Figure 6-1[a].

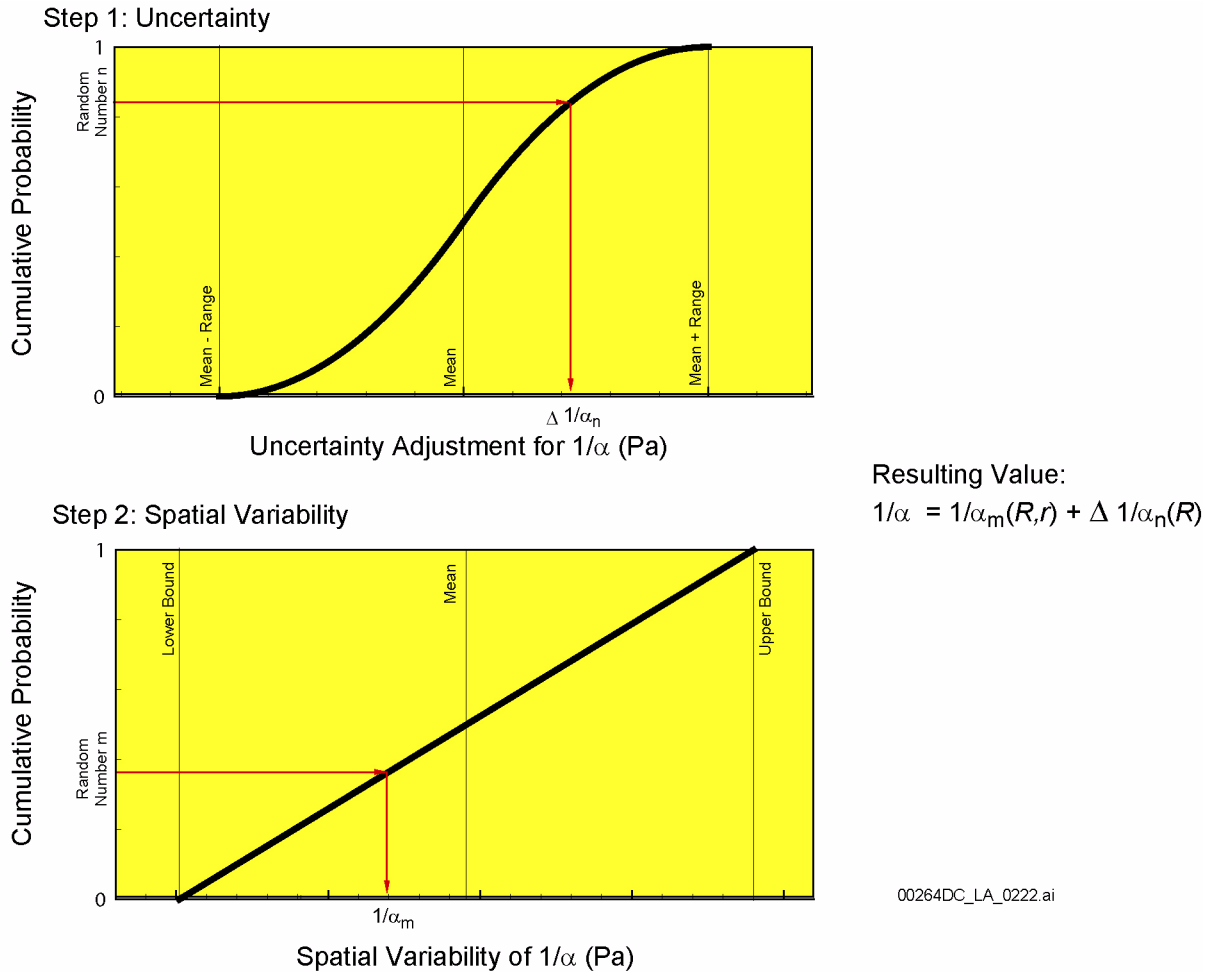

Figure 2.3.3-44. Schematic Illustration of Random Sampling Procedure for Capillary Strength Parameter, Using Cumulative Probability Distributions for Spatial Variability and Uncertainty

Source: SNL 2007a, Figure 6.5-2.

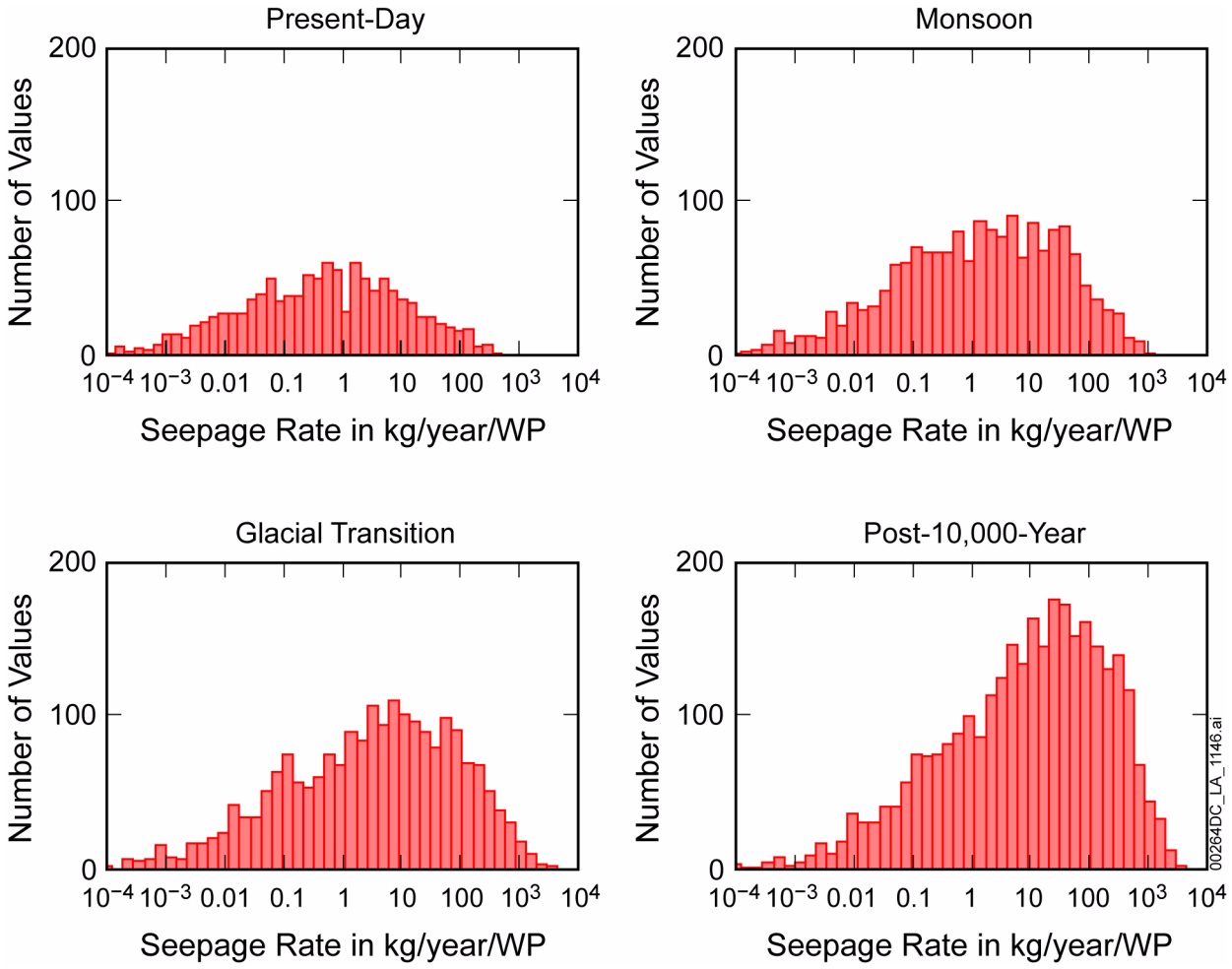

Figure 2.3.3-45. Histograms of Seepage Rates for Intact Drifts in Tptpll Unit

NOTE: Results for pre-10,000-year period were obtained using flow field from 10th percentile infiltration scenario. Results for post-10,000-year period were obtained using first flow field. These flow fields are the most likely ones of four with a relative occurrence probability of 62%. Only the samples with nonzero seepage are depicted.
WP = waste package.

Source: Modified from SNL 2007a, Figure 6-10[a].

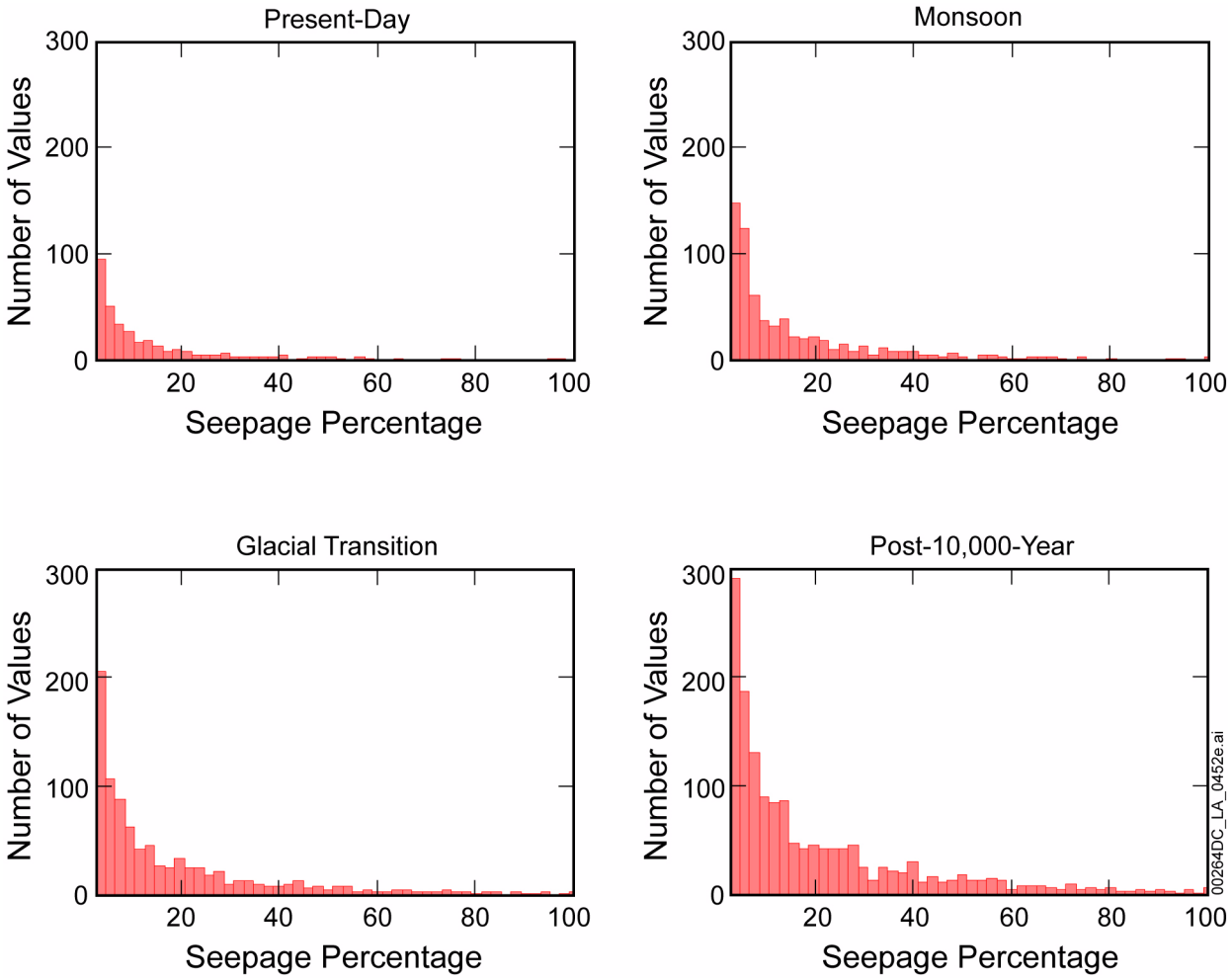

Figure 2.3.3-46. Histograms of Seepage Percentages for Intact Drifts in Tptpll Unit

NOTE: Results for pre-10,000-year period were obtained using flow field from 10th percentile infiltration scenario. Results for post-10,000-year period were obtained using first flow field. These flow fields are the most likely ones of four with a relative occurrence probability of 62%. Only the samples with nonzero seepage are depicted.

Source: Modified from SNL 2007a, Figure 6-11[a].

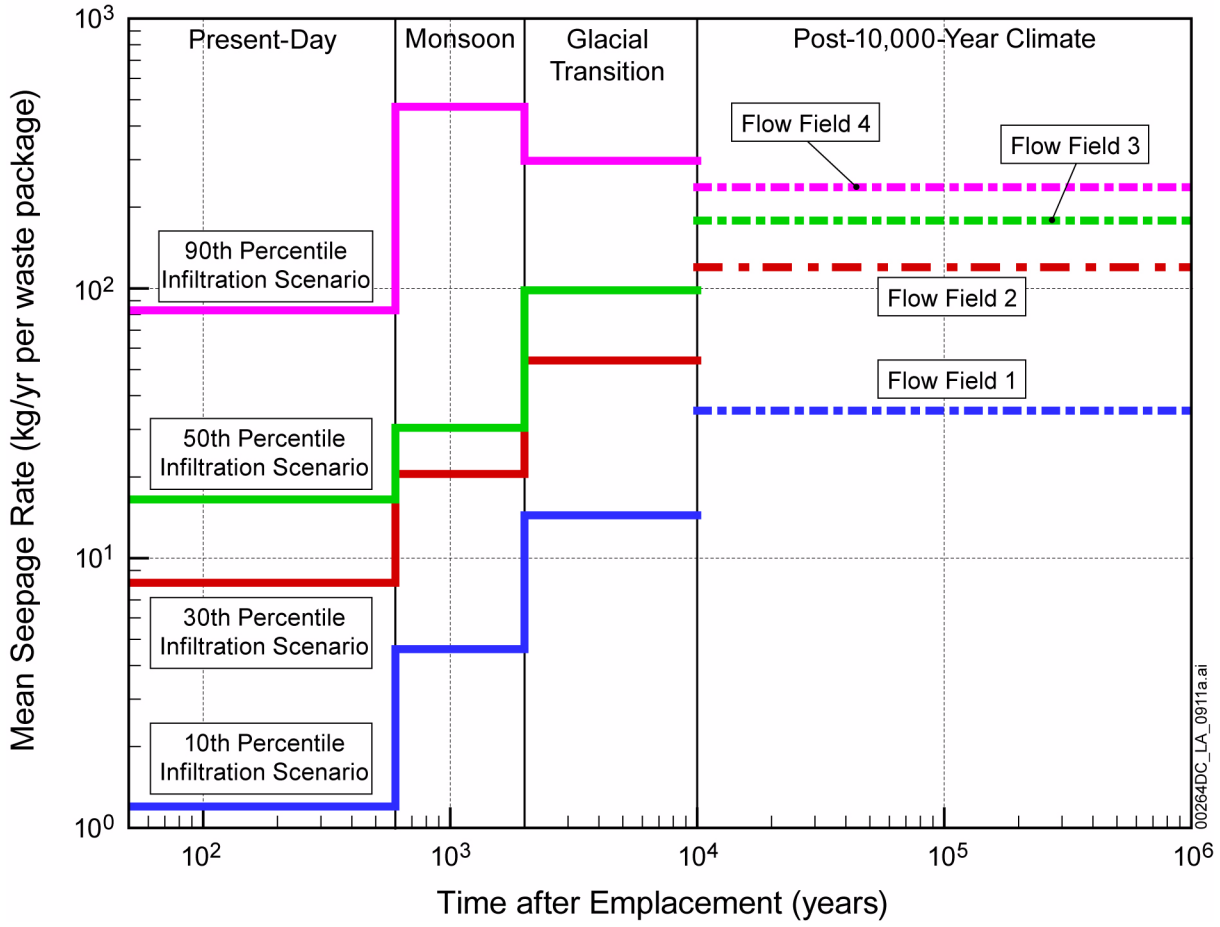

Figure 2.3.3-47. Mean Seepage Rate as a Function of Time After Emplacement for Intact Drifts in Tptpll Unit and Different Infiltration Scenarios

NOTE: Based on comparison of measured data from the unsaturated zone, weighting factors have been assigned that determine the relative occurrence probability of the flow fields related to different infiltration scenarios (Section 2.3.2). The four pre-10,000-year flow fields based on the 10th, 30th, 50th, and 90th percentile infiltration scenarios are associated with weighting factors of, respectively, 62%, 16%, 16%, and 6%. The four flow fields for the post-10,000-year period (flow fields 1 through 4) have the same weighting factors.

Source: SNL 2007a, Figure 6-13[a].

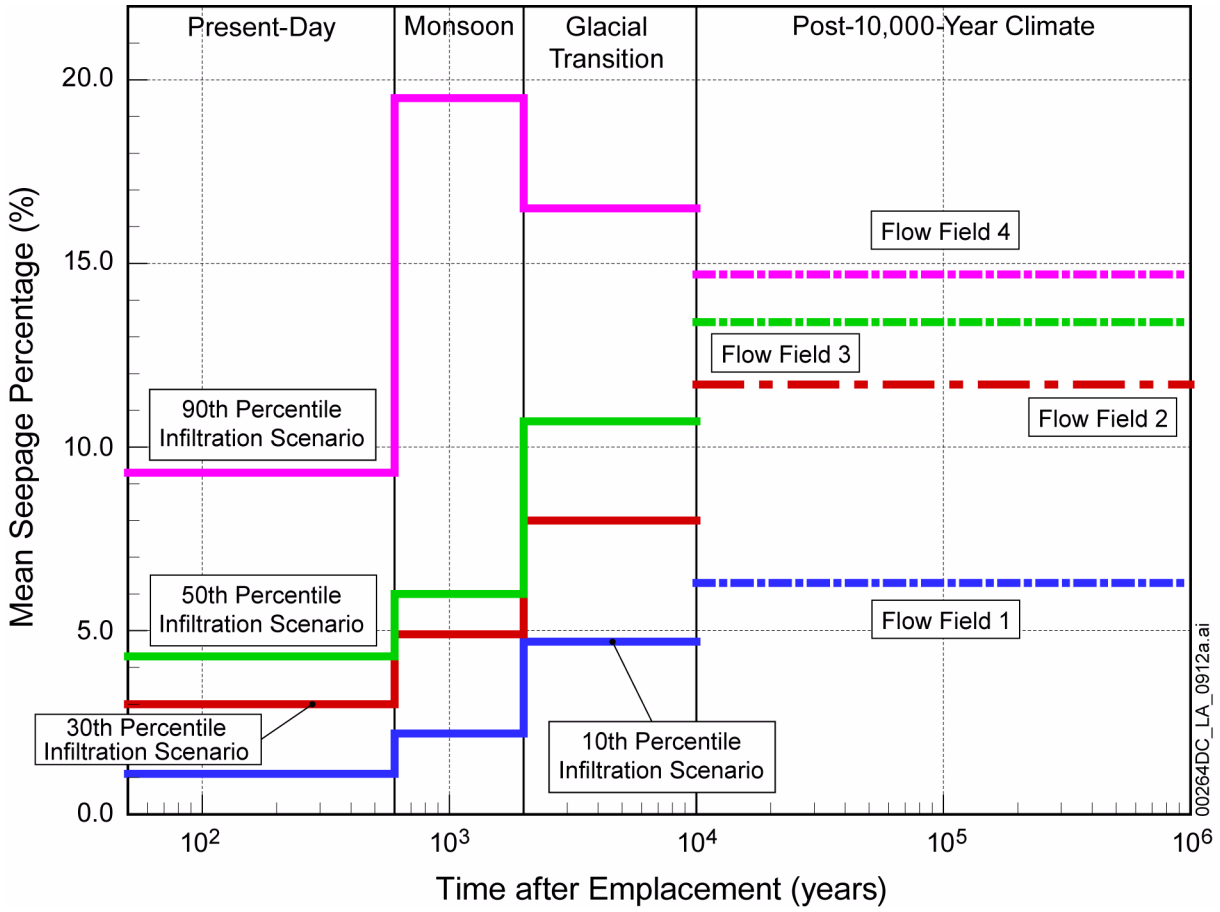

Figure 2.3.3-48. Mean Seepage Percentage as a Function of Time After Emplacement for Intact Drift in Tptpll Unit and Different Infiltration Scenarios

NOTE: Based on comparison of measured data from the unsaturated zone, weighting factors have been assigned that determine the relative occurrence probability of the flow fields related to different infiltration scenarios (Section 2.3.2). The four pre-10,000-year flow fields based on the 10th, 30th, 50th, and 90th percentile infiltration scenarios are associated with weighting factors of, respectively, 62%, 16%, 16%, and 6%. The four flow fields for the post-10,000-year period (flow fields 1 through 4) have the same weighting factors.

Source: SNL 2007a, Figure 6-14[a].

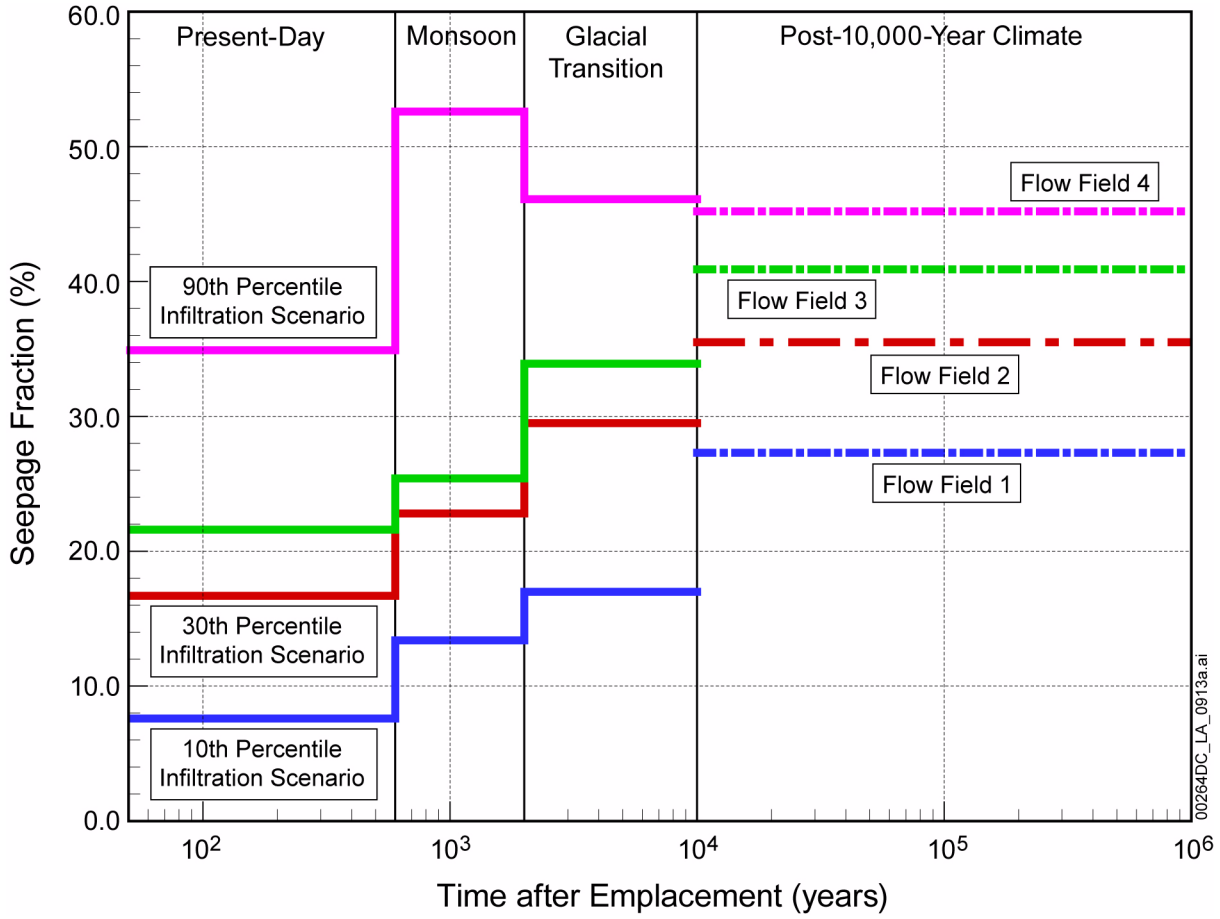

Figure 2.3.3-49. Seepage Fraction as a Function of Time After Emplacement for Intact Drift in Tptpll Unit and Different Infiltration Scenarios

NOTE: Based on comparison of measured data from the unsaturated zone, weighting factors have been assigned that determine the relative occurrence probability of the flow fields related to different infiltration scenarios (Section 2.3.2). The four pre-10,000-year flow fields based on the 10th, 30th, 50th, and 90th percentile infiltration scenarios are associated with weighting factors of, respectively, 62%, 16%, 16%, and 6%. The four flow fields for the post-10,000-year period (flow fields 1 through 4) have the same weighting factors.

Source: SNL 2007a, Figure 6-15[a].

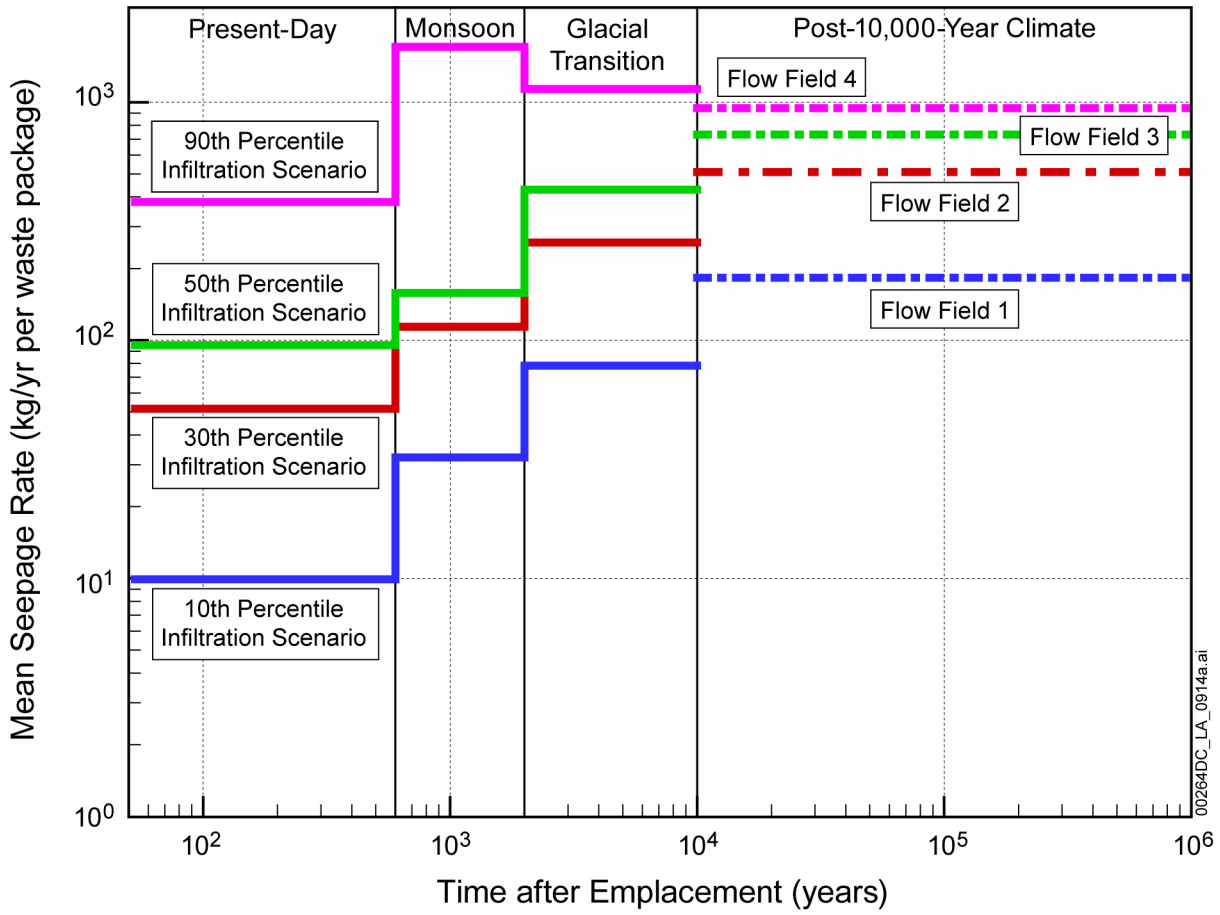

Figure 2.3.3-50. Mean Seepage Rate as a Function of Time After Emplacement for Collapsed Drift in Tptpll Unit and Different Infiltration Scenarios

NOTE: Based on comparison of measured data from the unsaturated zone, weighting factors have been assigned that determine the relative occurrence probability of the flow fields related to different infiltration scenarios (Section 2.3.2). The four pre-10,000-year flow fields based on the 10th, 30th, 50th, and 90th percentile infiltration scenarios are associated with weighting factors of, respectively, 62%, 16%, 16%, and 6%. The four flow fields for the post-10,000-year period (flow fields 1 through 4) have the same weighting factors.

Source: SNL 2007a, Figure 6-16[a].

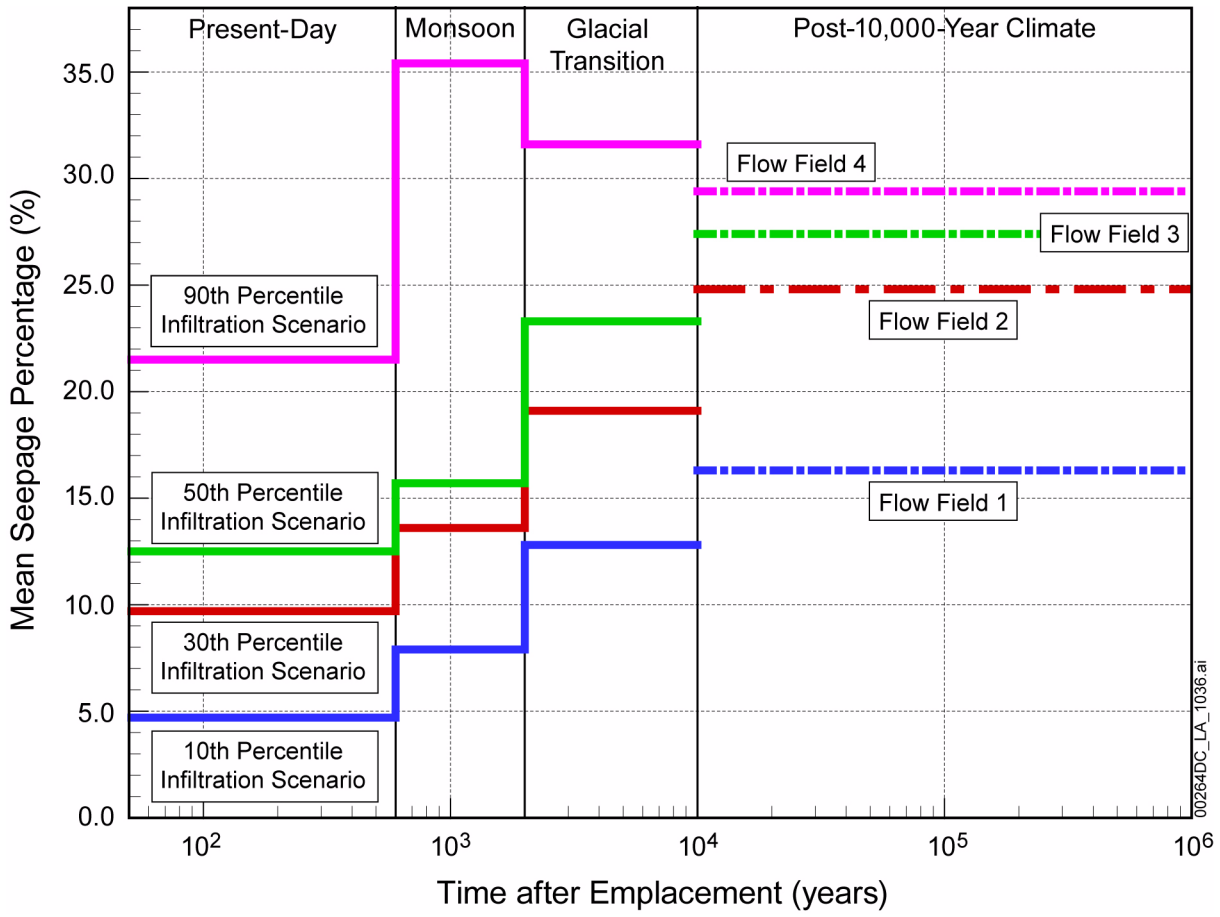

Figure 2.3.3-51. Mean Seepage Percentage as a Function of Time After Emplacement for Collapsed Drift in Tptpll Unit and Different Infiltration Scenarios

NOTE: Based on comparison of measured data from the unsaturated zone, weighting factors have been assigned that determine the relative occurrence probability of the flow fields related to different infiltration scenarios (Section 2.3.2). The four pre-10,000-year flow fields based on the 10th, 30th, 50th, and 90th percentile infiltration scenarios are associated with weighting factors of, respectively, 62%, 16%, 16%, and 6%. The four flow fields for the post-10,000-year period (flow fields 1 through 4) have the same weighting factors.

Source: SNL 2007a, Figure 6-17[a].

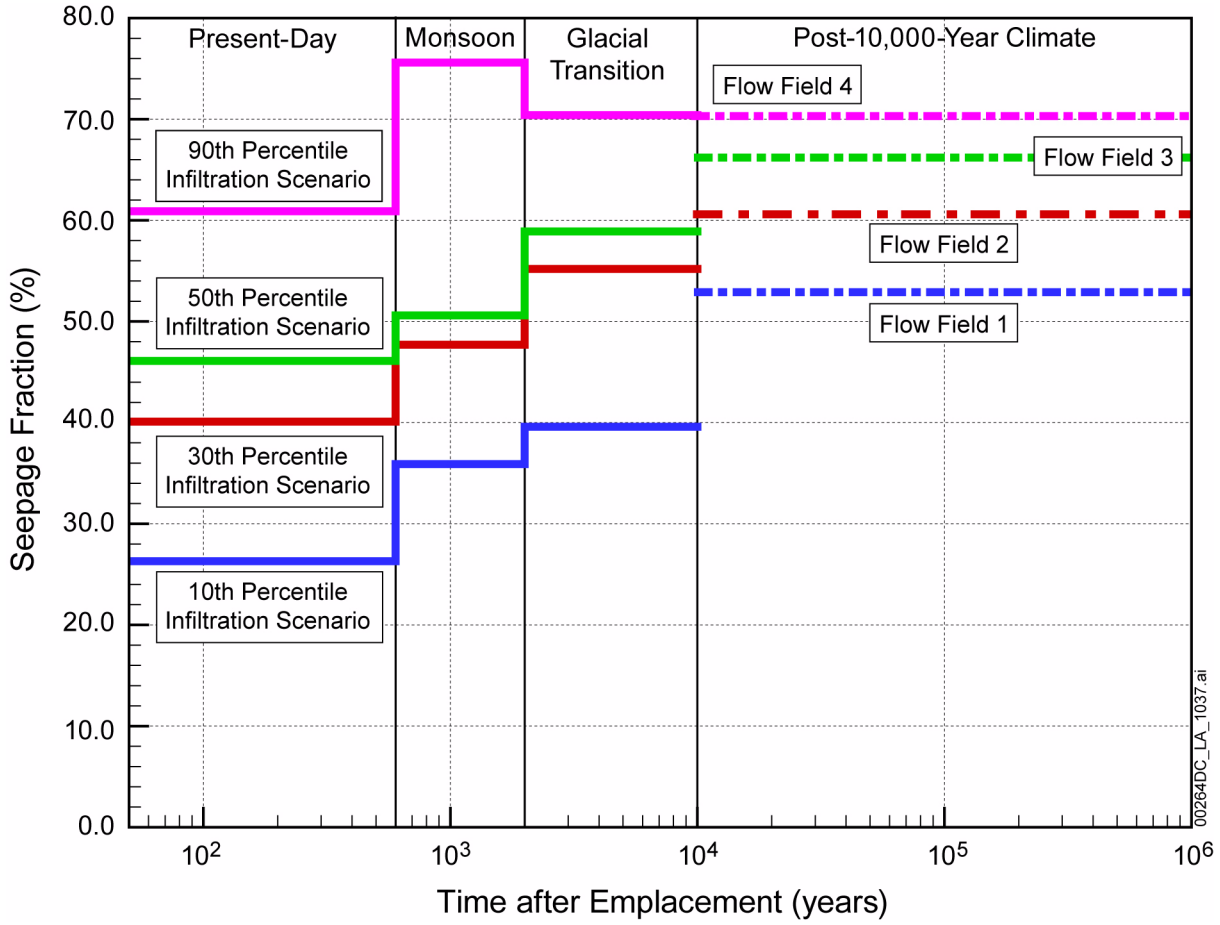

Figure 2.3.3-52. Seepage Fraction as a Function of Time After Emplacement for Collapsed Drift in Tptpll Unit and Different Infiltration Scenarios

NOTE: Based on comparison of measured data from the unsaturated zone, weighting factors have been assigned that determine the relative occurrence probability of the flow fields related to different infiltration scenarios (Section 2.3.2). The four pre-10,000-year flow fields based on the 10th, 30th, 50th, and 90th percentile infiltration scenarios are associated with weighting factors of, respectively, 62%, 16%, 16%, and 6%. The four flow fields for the post-10,000-year period (flow fields 1 through 4) have the same weighting factors.

Source: SNL 2007a, Figure 6-18[a].